Density functional theory for spherical drops

1994 J. Phys.: Condens. Matter 6 5303

(http://iopscience.iop.org/0953-8984/6/28/008)

J. Phys.: Condens. Matter 6 (1994) 5303–5322. Printed in the UK

Density functional theory for spherical drops

Ioannis Hadjiagapiou

Solid State Physics Section, Department of Physics, University of Athens, Panepistimiopolis, Zografos GR 157 84, Athens, Greece

Received 3 December 1993, in final form 8 April 1994

Abstract. We have applied Sullivan's model to study the interfacial properties of a spherical drop embedded in a one-component fluid using the mean field approximation. We have examined the effect of drop size (expressed by the equimolar radius R_e) on the density profile, pressure tensor, pressure difference Δp across the interface, surface tension, Tolman's length, and density, pressure, and normal component of pressure tensor at the centre of the drop. Δp is found to be an ill defined quantity in the sense that it can be defined in various ways, whose results coincide for large drops. The surface tension is a non-monotonic function of R_e; it increases slowly from its flat interface value as R_e decreases until a maximum value is attained, then it decreases rapidly. For small supersaturations, the drops are under tension and compression while at large supersaturations they are only under tension. The results of this theory are compared qualitatively with previous molecular dynamics simulations and theoretical calculations for drops.

1. Introduction

The statistical mechanics of curved interfaces, mainly spherical and cylindrical, is equally important as (if not more important than) that of planar interfaces, but it needs a more subtle analysis than the flat geometry wherein much progress has been achieved in understanding its statistical mechanical properties [1–3]; although the theory of curved interfaces was founded on sound thermodynamic arguments, late in the 1940s [1, 4, 27], it has received little attention. Non-planar interfaces are involved in many circumstances, e.g. oil recovery, homogeneous nucleation, pollution technology, etc, thus a detailed understanding of the curvature dependence of the interfacial properties of curved interfaces (which are still not satisfactorily understood) is important. Here we examine spherical fluid interfaces embedded in a one-component vapour background.

The early studies of the influence of curvature on the properties of drops date back to Young and Laplace in the nineteenth century. Laplace considered a drop of radius R enclosing a homogeneous liquid-like phase (interior phase) separated from a homogeneous bulk vapour phase (exterior phase) by a mathematical dividing surface where the density changes abruptly from its constant value inside the drop to its constant value outside; the drop, to be stable against the surface tension γ (regarded as a mechanical force) of the vapour–liquid interface, must set up a pressure difference Δp over the interface to balance the contracting force and maintain the system in equilibrium; the condition of mechanical equilibrium, called the Laplace law, is

$$\Delta p = 2\gamma/R \tag{1.1}$$

where $\Delta p = p_l - p_v$ is the pressure difference between the pressure p_l of the interior phase and p_v the pressure of the exterior; these pressures can be identified as 'bulk' pressures in

0953-8984/94/285303+20$19.50

the centre of the drop and far outside the drop, since the drop is considered to be large so that the interior phase is homogeneous (constant interior density ϱ_l). However, the exact numerical value of γ is not specified, but γ is considered to be equal asymptotically to its planar value γ_∞ as the drop grows.

Gibbs was the first to treat the spherical liquid interface on the basis of thermodynamics regarding this inhomogeneous system as consisting of a homogeneous interior phase (bulk-like liquid) separated from the exterior bulk vapour phase by an arbitrary mathematical spherical dividing surface possessing a radius-dependent tension $\gamma(R)$ and an excess mass density Γ_s [1,4]. Gibbs introduced the notion of the surface of tension (with radius R_s and associated surface tension $\gamma_s = \gamma(R_s)$) such that the Laplace equation retains its form, i.e.,

$$\Delta p = 2\gamma(R_s)/R_s \tag{1.2}$$

and for which the curvature coefficient $C(R)$ vanishes ($C(R) = A[\mathrm{d}\gamma/\mathrm{d}R]$; A is the area of the dividing surface with radius R and associated surface tension γ; the brackets denote changes following from a notional change in the position of the dividing surface and not a physical change in the state of the system). Another dividing surface, introduced by Gibbs, is the so-called equimolar dividing surface with radius R_e and associated surface tension γ_e; this choice makes the excess surface density Γ_s vanish. We further introduce another surface at $r = R_{max}$ where the absolute value of the first derivative of the number density $\varrho(r)$ with respect to the distance r from the origin of the drop becomes maximum; the associated surface tension is γ_{max}. In any case, the dividing surfaces are introduced solely for computational convenience and the values of the observable quantities such as R, p_l, p_v, and μ (chemical potential) must be independent of the particular choice (for fixed N, V and T), while the value of the surface tension depends on the choice of the dividing surface.

Tolman, on thermodynamics grounds, extended Gibbs theory to obtain the radius dependence of surface tension [4]

$$\frac{\gamma(R)}{\gamma(\infty)} = 1/(1 + 2\delta/R) \tag{1.3}$$

that is

$$\frac{\gamma(R)}{\gamma(\infty)} \cong 1 - 2\delta/R + \mathrm{O}(1/R^2). \tag{1.4}$$

Tolman introduced the new parameter δ (known as Tolman's length)

$$\delta = \lim_{R_e \to \infty} (R_e - R_s) = z_e - z_s \tag{1.5}$$

where z_e and z_s are the equimolar and surface of tension dividing surfaces for the flat interface, respectively. Laplace's equation (1.2) must now be modified to include the first-order correction through the Tolman length δ

$$\Delta p = (2\gamma/R)(1 - \delta/R). \tag{1.6}$$

Δp is a unique function of T and μ and does not depend on the choice of the dividing surface.

The mechanical and thermodynamic routes to the surface tension, although successful in calculating it for large drops, are inappropriate for small radii and fail to predict microscopic properties such as the structure and stress in the interfacial region. In addition, for small drops, the uniform liquid phase inside the drop, a necessary ingredient of these two routes, departs from the actual state prevailing inside a small drop, because in computer simulations [6] it was found that in small drops the density is non-uniform up to the centre of the drop and the surface tension deviates from the flat interface value. Such small systems can be described by statistical mechanics of inhomogeneous fluids together with an appropriate molecular model.

Guermeur *et al* [10] found that the surface tension exhibits a non-monotonic behaviour in contrast to the monotonic one (it decreases as the drop radius decreases) found in [11], [14], and [20]; the latter behaviour is in agreement with the computer simulation of Thompson *et al* [6]. Another interfacial quantity studied is Tolman's length δ, which has caused much debate. Guermeur *et al* [10] found that it is negative for $R_s > 25.06$ Å and positive for equal or smaller R_s values while in [11] and [14] δ is positive and increases as the drop radius decreases; however, in numerical simulation its behaviour is not clear [6, 15, 21]. Falls *et al* [14] also calculated the pressure tensor components $p_N(r)$, and $p_T(r)$ (the normal and transverse respectively), finding that all the drops they had considered, irrespective of their size, initially, are under tension ($p_T(r) < p_N(r)$) but later are under compression ($p_T(r) > p_N(r)$), while in computer simulation [6, 15] this behaviour was not detected.

It seems from the previous discussion that there are many problems concerning the various interfacial quantities; we study, in detail, the interfacial properties of a one-component drop immersed in a vapour background (temperature T) using Sullivan's model [8] and a suitable grand canonical functional. Sullivan's model was applied successfully to planar interface fluids (one-component and binary mixtures [2, 8, 28–30]). Here this model is applied to drops of various sizes at reduced temperature $T^* = T/T_c = 0.8$, where T_c is the critical temperature of the fluid. After the calculation of the density profile as a function of the distance from the centre of the drop, the various interfacial quantities (e.g., pressure tensor, surface tension, etc) are evaluated. These results are compared with other numerical and molecular dynamics (MD) calculations [6, 15, 21] based on other models and approximations, because of the lack of experimental results on spherical drops. The paper is arranged as follows. In section 2, we outline the mean field theory (MFT) for a spherical interface and derive the relevant differential equation with the proper boundary conditions. Section 3 is devoted to the discussion of the pressure tensor, the mechanical and thermodynamic routes to the surface tension, and its associated radius. In section 4, we present the results of the numerical calculations of density profiles and the interfacial functions. In section 5, we discuss our results and compare them with others. The model we have adopted is that of a model fluid of attracting hard spheres with diameter d.

2. Theory

We consider a one-component non-uniform system, comprising a liquid drop (of radius R) and a vapour background; the grand potential functional of this system, in the absence of an external field, is

$$\Omega_V[\varrho(r)] = \int_V \mathrm{d}r \left\{ f_h[\varrho(r)] + \tfrac{1}{2}\varrho(r) \int \varrho(r')w(|r-r'|)\,\mathrm{d}r' - \mu\varrho(r) \right\} \tag{2.1}$$

where $\varrho(r)$ is the average number density at point r, μ the bulk vapour phase chemical potential and V the volume of the system. The repulsive force contribution to the Helmholtz free energy is treated in the local density approximation in that $f_h[\varrho(r)]$ is the Helmholtz free energy density of a uniform hard-sphere fluid at density $\varrho(r)$, while the long-range attractive forces are treated in the mean field approximation so that $w(r)$ is the attractive part of the pairwise potential between two fluid molecules [1,7].

The equilibrium density $\varrho(r)$ is that minimizing the functional (2.1) and by setting $\delta\Omega[\varrho(r)]/\delta\varrho(r) = 0$, the Euler–Lagrange equation results:

$$\mu = \mu_h[\varrho(r)] + \int w(|r - r'|)\varrho(r')\,dr' \tag{2.2}$$

where $\mu_h[\varrho(r)] = \partial f_h[\varrho(r)]/\partial\varrho(r)$ is the hard-sphere chemical potential; when (2.2) is substituted into (2.1) the equilibrium grand potential Ω_V results. The integral equation (2.2) can be converted to a non-linear second-order differential equation by choosing properly the interaction potential [8]

$$w(r) = -(\alpha\lambda^3/4\pi)e^{-\lambda r}/\lambda r \tag{2.3}$$

where λ is an inverse range length such that $\lambda d = 1$ and α is given by

$$\alpha = -\int w(r)\,dr. \tag{2.4}$$

Assuming spherically symmetric solutions, $\varrho(r) = \varrho(r)$, to (2.2) and that the centre of the drop coincides with the origin of the coordinate axes, the integration in (2.2) over the polar angles θ and φ can be done analytically,

$$\mu = \mu_h(u) - \frac{\alpha}{2u}\int_0^\infty u'\rho(u')[e^{-|u-u'|} - e^{-|u+u'|}]\,du' \tag{2.5}$$

where $u = \lambda r$, the dimensionless radial distance from the centre of the drop, and if the integral equation (2.5) is differentiated twice with respect to u it yields

$$d^2\mu_h(u)/du^2 + (2/u)\,d\mu_h(u)/du - \mu_h(u) + \mu = -\alpha\varrho(u). \tag{2.6}$$

This equation is similar to that in the flat geometry [8] apart from the second term in the left-hand side, which causes significant complications in the behaviour of the system and needs a subtle analysis. The solution to (2.6) is uniquely defined if this is supplemented by proper boundary conditions so that its solution represents a real system. We examine the behaviour of the solution in the two limiting cases as $u \to 0$ and $u \to \infty$. As the distance u becomes larger the contribution of the term $(2\mu_h'(u)/u)$ becomes less significant, so the behaviour of the density profile $\varrho(r)$ is similar to that of the one-dimensional planar interface at the same temperature [8]; thus one of the boundary conditions is that $\mu_h(u)$ approaches $\mu_h^v = \mu_h(\varrho_{vs})$ (the hard-sphere chemical potential of the bulk vapour with density ϱ_{vs}) as $u \to \infty$.

However, as u approaches the centre of the drop, $u = 0$, the solution is less well behaved, since at the origin $u = 0$ (2.6) is singular if $\mu_h'(u)$ remains non-zero in the limit $u \to 0$; $\mu_h''(u)$ will diverge in this limit and the solution $\mu_h(u)$ will be singular. However, this singularity can be removed if $\mu_h'(u)$ vanishes as u approaches zero, thus

$$\lim_{u\to 0}\frac{\mu_h'(u)}{u} = \lim_{u\to 0}\frac{d\mu_h'(u)/du}{du/du} = \lim_{u\to 0}\mu_h''(u) \tag{2.7}$$

according to the l'Hopital rule. Therefore, in the neighbourhood of the origin (2.6) becomes

$$\lim_{u\to 0}\mu_h''(u) = \tfrac{1}{3}(\mu_h(u) - \mu - \alpha\rho(u)). \tag{2.8}$$

As the drop becomes increasingly larger, the density at the centre of the drop, $\varrho(0)$, approaches asymptotically a constant value that is very nearly equal to ϱ_{ls} (the density of a uniform liquid with the system's chemical potential $\mu(\varrho_{ls}) = \mu$, i.e., ϱ_{ls} is one of the solutions of $\mu(\varrho) - \mu = 0$; the other is ϱ_{vs}) and the larger the drop, the closer $\varrho(0)$ to ϱ_{ls}, but when the radius R of the drop is small, then $\varrho(0)$ departs significantly from ϱ_{ls} and becomes smaller. The other boundary condition is the vanishing of $\mu_h'(u)$ at $u = 0$, i.e., $\mu_h'(0) = 0$, so that the solution at $u = 0$ is bounded.

The crucial point is the calculaiton of the density profile that results as a solution of the previous boundary value problem (2.6); however, instead of solving (2.6) for the hard-sphere chemical potential $\mu_h(u)$ (a monotonically increasing function of density $\varrho(u)$), this equation was transformed into an equation for the packing fraction $\eta = \pi d^3\varrho/6$ by adopting the Carnahan–Starling approximation for the hard spheres, i.e.,

$$\mu_h(\eta) = k_B T(\ln\eta + (8\eta - 9\eta^2 + 3\eta^3)/(1-\eta)^3) \tag{2.9}$$

for the hard-sphere chemical potential, while the hard-sphere pressure is

$$p_h(\eta) = k_B T\varrho(1 + \eta + \eta^2 - \eta^3)/(1-\eta)^3 \tag{2.10}$$

where k_B is the Boltzmann constant.

Substitution of (2.9) into (2.6) gives,

$$\eta''(u) = -(2/u)\eta'(u) - B_1(\eta)\eta'^2(u) - B_2(\eta) - B_3(\eta)\eta(u) \tag{2.11}$$

for $u \neq 0$ and

$$\begin{aligned} A_1 &= \partial(\beta\mu_h)/\partial\eta = 1/\eta + (8-2\eta)/(1-\eta)^4 \\ A_2 &= \partial A_1/\partial\eta = -1/\eta^2 + (30-6\eta)/(1-\eta)^5 \end{aligned} \tag{2.12a}$$

$$\begin{aligned} B_1(\eta) &= A_2(\eta)/A_1(\eta) \\ B_2(\eta) &= [\beta\mu - \beta\mu_h(u)]/A_1(\eta) \\ B_3(\eta) &= 6\alpha\beta/\pi A_1(\eta) \end{aligned} \tag{2.12b}$$

subject to the boundary conditions

$$\eta'(0) = 0 \qquad \eta(\infty) = \eta_v \qquad \eta'(\infty) = 0 \tag{2.13}$$

where $\beta = (k_B T)^{-1}$.

In the neighbourhood of the centre of the drop, the solution is expanded in power series about $u = 0$ [9]

$$\eta(u) = \eta(0) + (u^2/2)\eta^{(2)}(0) + (u^3/3!)\eta^{(3)}(0) + (u^4/4!)\eta^{(4)}(0) + \cdots. \tag{2.14}$$

Substituting (2.14) into (2.11), the coefficients $\eta^{(i)}(0)$, $i = 2, 3, 4, \ldots$ can be expressed in terms of the unknown value $\eta(0) = q$ of the packing fraction at the origin $u = 0$,

$$\eta^{(2)}(0) = -\tfrac{1}{3}[B_2(q) + qB_3(q)] \tag{2.15a}$$

$$\eta^{(3)}(0) = 0 \tag{2.15b}$$

$$\eta^{(4)}(0) = -\tfrac{3}{5}\left\{2B_1(q)[\eta^{(2)}(0)]^2 + \eta^{(2)}(0)\left[\left(\frac{\mathrm{d}B_2(\eta)}{\mathrm{d}\eta}\right)_{u=0} + q\left(\frac{\mathrm{d}B_3(\eta)}{\mathrm{d}\eta}\right)_{u=0} + B_3(q)\right]\right\} \tag{2.15c}$$

thus the solution (2.14) becomes

$$\eta(u) = q + (u^2/2!)\eta^{(2)}(0) + (u^4/4!)\eta^{(4)}(0). \tag{2.16}$$

For the subsequent calculations all the quantities and equations are transformed to dimensionless 'reduced' units:

$$\begin{aligned} &\mu^* = \mu/k_\mathrm{B}T \qquad p^* = d^3p/k_\mathrm{B}T \qquad T^* = T/T_\mathrm{c} \qquad u = r/d \\ &\gamma^* = d^2\gamma/k_\mathrm{B}T \qquad \varrho^* = \varrho d^3 \qquad \alpha^* = \alpha/(k_\mathrm{B}Td^3) = 11.102/T^* \end{aligned} \tag{2.17}$$

thus

$$\mu^*(\varrho^*, T^*) = \mu_\mathrm{h}^*(\varrho^*, T^*) - \alpha^*\varrho^* \tag{2.18a}$$

$$p^*(\varrho^*, T^*) = p_\mathrm{h}^*(\varrho^*, T^*) - \alpha^*\varrho^{*2}/2 \tag{2.18b}$$

although the asterisks, for simplicity in the expressions, will be suppressed, all the results will be with respect to the dimensionless variables (2.17).

Initially, the coexisting bulk densities ϱ_vc and ϱ_lc, together with the corresponding spinodal ones ϱ_vsp and ϱ_lsp are obtained, for various temperatures T, by solving the simultaneous equations

$$p(\varrho_\mathrm{vc}) = p(\varrho_\mathrm{lc}) \qquad \mu(\varrho_\mathrm{vc}) = \mu(\varrho_\mathrm{lc}) \tag{2.19}$$

for the densities ϱ_vc and ϱ_lc, and the equations

$$\mu'(\varrho_\mathrm{vsp}) = 0 \qquad \mu'(\varrho_\mathrm{lsp}) = 0 \tag{2.20}$$

for the spinodal densities ϱ_vsp and ϱ_lsp. The equilibrium density profile for the planar interface was obtained by numerically solving the corresponding equation for the free interface [8]

$$\mathrm{d}\mu_\mathrm{h}(x)/\mathrm{d}x = -[(\mu_\mathrm{h}(x) - \mu)^2 - 2\alpha(p_\mathrm{h}(x) - p)]^{1/2} \tag{2.21}$$

for the reduced temperature $T^* = 0.8$ and coexisting densities $\varrho_\mathrm{vc} = 0.041\,478\,6$, $\varrho_\mathrm{lc} = 0.586\,731\,6$, (see figure 1; the zero of the x-axis was chosen deep in the liquid phase where $\mu_\mathrm{h}(\varrho_\mathrm{lc}) = \mu_\mathrm{h}^\mathrm{lc}$), also the corresponding surface tension was calculated from the formula

$$\gamma_\infty = \frac{1}{\alpha}\int_0^\infty [\mu_\mathrm{h}'(x)]^2\,\mathrm{d}x = \frac{1}{\alpha}\int_{\mu_\mathrm{h}^\mathrm{v}}^{\mu_\mathrm{h}^\mathrm{l}} \mu_\mathrm{h}'(x)\,\mathrm{d}\mu_\mathrm{h} \tag{2.22}$$

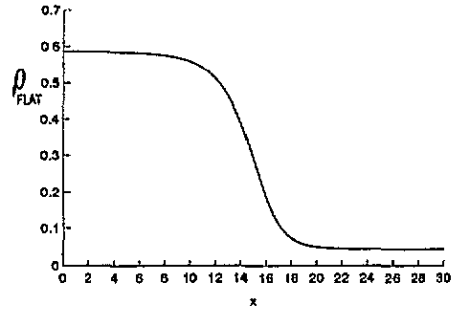

Figure 1. The density profile for flat geometry and $T^* = 0.8$.

and it was found to be equal to 0.440 094 8.

A one-component two-phase system separated by a planar interface has only one degree of freedom according to the Gibbs phase rule, usually chosen as the temperature T, while a system comprising a spherical drop and bulk vapour has another, which is the parameter controlling the size of the drop; as such a parameter we choose the density ϱ_{vs} of the homogeneous bulk vapour phase surrounding the drop (this is not the only choice), which can take any value within the interval $(\varrho_{vc}, \varrho_{vsp})$. The curvature influences not only the various interfacial quantities but the bulk ones, as well. The bulk vapour phase is supersaturated, yielding a larger bulk vapour density, ϱ_{vs}, than is the case with the planar geometry (density ϱ_{vc}); also the pressures p_v and p_l of the bulk vapour phase and the corresponding liquid, respectively, are not equal, in contrast to what happens in the planar geometry. The equilibrium (at temperature T) between a liquid and its vapour in the case of a planar dividing surface is achieved by the equality of their chemical potentials and pressures (relations (2.19)), while for the spherical interface, at equilibrium, only the chemical potentials are equal and not the pressures (see Laplace equation (1.1)).

3. Pressure tensors

In any homogeneous phase, the pressure is uniform (scalar quantity), hence, in the case of a two-phase system, in the interior of either homogeneous phase the pressure tensor (the negative of the microscopic stress tensor) reduces to the bulk pressure p multiplied by the unit tensor $\mathbf{I}$. However, within the interfacial region the force acting across a unit area is not the same in different directions since the physical interface is of finite thickness and the density varies considerably with position within this layer; consequently, the pressure tensor also varies. The pressure tensor $\mathbf{p}(r)$ consists of an isotropic part, which is well defined, and a configurational part, which is not (thus introducing the arbitrariness into the definition of $\mathbf{p}(r)$ [1, 12, 13, 21]. Recently, Baus and Lovett claimed that this ambiguity can be eliminated by imposing on $\mathbf{p}(r)$ St Venant's condition so that $\mathbf{p}(r)$ is well defined [23]; Rowlinson, in a subsequent letter [24], argued that this condition implies a vanishing surface tension; in a counterargument Baus and Lovett [25] commented on the validity of their argument; however, the matter is still unclear. The drop is in mechanical equilibrium expressed by the equation (in the absence of any external field)

$$\nabla \cdot \mathbf{p}(r) = \mathbf{0}. \tag{3.1}$$

For a planar dividing surface (coinciding with the xy-plane) in the interfacial layer p_{xy}, p_{yz} and p_{zx} vanish, while $p_{xx}(z) = p_{yy}(z) = p_T(z)$ and $p_{zz}(z) = P_N(z) = p_{flat}$ (bulk pressure), thus the pressure tensor, in this case, is written

$$\mathbf{p}(z) = p_T(z)(\hat{e}_x\hat{e}_x + \hat{e}_y\hat{e}_y) + p_N(z)\hat{e}_z\hat{e}_z \tag{3.2}$$

where $(\hat{e}_x, \hat{e}_y, \hat{e}_z)$ is the orthonormal set in Cartesian coordinates. The tangential component $p_T(z)$ may vary in a complicated way depending only on z (due to symmetry), while the normal component $p_N(z)$ remains constant even in the transition layer.

In the case of a spherical interface the pressure tensor $\mathbf{p}(r)$, on grounds of symmetry (see [1] and [26]), will depend only on the radial distance r and consists of a transverse part $p_T(r)$ and a radial one $p_N(r)$, i.e.

$$\mathbf{p}(r) = p_N(r)[\hat{e}_r\hat{e}_r] + p_T(r)[\mathbf{I} - \hat{e}_r\hat{e}_r] \tag{3.3}$$

where $\mathbf{I}$ is the (3×3) unit tensor. Now, the normal component $p_N(r)$ is no longer a constant but varies with the distance from the origin of the drop as determined by (3.1). Substitution of (3.3) into (3.1) gives the result

$$p_N'(r) = (2/r)[p_T(r) - p_N(r)] \tag{3.4}$$

where the prime denotes the derivative with respect to r. Equation (3.4), on the one hand, can be integrated from inside to outside,

$$p_N(0) - p_N(\infty) = 2\int_0^\infty \frac{[p_N(r) - p_T(r)]}{r}\,dr. \tag{3.5}$$

The left-hand side of (3.5) can be considered as one of the possible definitions of the pressure difference Δp (see below (3.17)). On the other hand, (3.4) can be regarded as a differential equation for $p_N(r)$, once $p_T(r)$ is known, i.e.

$$(r/2)\mathrm{d}p_N(r)/\mathrm{d}r + p_N(r) = p_T(r) \tag{3.6}$$

which, when integrated, yields the result

$$p_N(r) = \frac{2}{r^2}\int_0^r p_T(r_1)r_1\,dr_1. \tag{3.7}$$

The Helmholtz free energy F as well as the grand potential Ω are independent of the choice of the position of the dividing surface; as a consequence we have [1]

$$\Delta p = p_l - p_v = 2\gamma/R_\gamma + [\mathrm{d}\gamma/\mathrm{d}R_\gamma] \tag{3.8a}$$

$$C = A[\mathrm{d}\gamma/\mathrm{d}R_\gamma] \tag{3.8b}$$

where R_γ is the radius of the dividing surface and C the coefficient of the curvature term. The relation (3.8a) is a generalization of the Laplace equation to allow for higher-order curvature corrections.

The surface excess density is given by the relation [1]

$$\Gamma(R) = \frac{N_s}{4\pi R^2} = \frac{1}{R^2}\left\{\int_0^R [\rho(r) - \rho_{ls}]r^2\,dr + \int_R^\infty [\rho(r) - \rho_{vs}]r^2\,dr\right\} \tag{3.9}$$

where N_s is the surface number of molecules.

The dividing surfaces are chosen to lie inside the interfacial region and satisfy special properties concerning interfacial quantities. The first dividing surface is that for which

$$C(R) = 0 \tag{3.10a}$$

or, equivalently,

$$p_l - p_v = 2\gamma(R_s)/R_s \tag{3.10b}$$

that is, the one for which Laplace's equation preserves its form and is called the surface of tension; its radius is R_s. Comparing (3.10*a*) with (3.8*b*) we see that this dividing surface minimizes the surface tension.

We now proceed to calculate the various interfacial functions (pressure tensor, surface tension and associated radius) for the model fluid under consideration (2.1,3).

$p_T(r)$ can be identified with minus the grand potential free energy density [26], i.e.

$$p_T(r) = -\omega_0[\varrho(r)]. \tag{3.11}$$

If the Euler–Lagrange equation (2.2) is substituted into the grand potential functional (2.1), the equilibrium grand potential $\Omega_V[\varrho_0(r)]$ results,

$$\Omega_V[\varrho_0(r)] = -\int \left\{ p_h(\varrho_0(r)) + \tfrac{1}{2}\varrho_0(r) \int dr' \, \varrho_0(r') w(|r - r'|) \right\} dr \tag{3.12}$$

where $\varrho_0(r)$ is the equilibrium density; accordingly (3.11) can be rewritten

$$p_T(r) = p_h(\varrho_0(r)) + \frac{1}{2}\varrho_0(r) \int \varrho_0(r') w(|r - r'|) \, dr'. \tag{3.13}$$

The pressure tensor components $p_T(r)$ and $p_N(r)$ are different in the interfacial region; in the homogeneous bulk vapour phase they are identical and coincide with the bulk vapour pressure

$$p_T(\infty) = p_N(\infty) = p_v = p(\rho_{vs}) \tag{3.14}$$

as can be verified from (3.6) and (3.13). Also these two components are identical at the centre of the drop $u = 0$,

$$p_T(0) = p_N(0) = p_h(0) + \tfrac{1}{2}\varrho_0(0) \int \varrho_0(r') w(|r'|) \, dr' \tag{3.15}$$

thus, if the drop is large enough, the interior phase possesses a uniform part, $p_T(0)$, $p_N(0)$ and $p(0)$ tend asymptotically to the pressure $p_l = p(\varrho_{ls})$, which corresponds to that of a uniform liquid phase of density ϱ_{ls} such that $\mu(\varrho_{ls}) = \mu(\varrho_{vs})$; otherwise, the interior phase

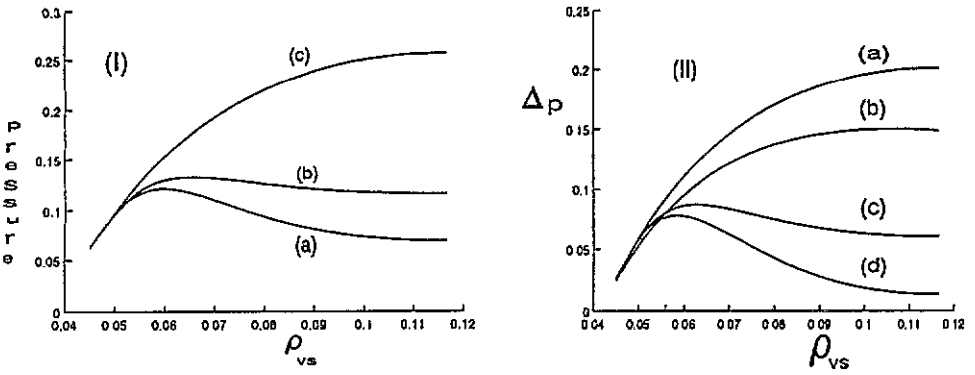

Figure 2. (I) Variation of the pressure at the drop centre, $p(\varrho(0))$ (*a*), the normal component of the pressure tensor at the drop centre, $p_N(\varrho(0))$ (*b*), and the pressure at density ϱ_{ls} (*c*), with respect to bulk vapour density ϱ_{vs}. (II) Pressure difference Δp against bulk vapour density ϱ_{vs}: $p(\varrho_{ls}) - p(\varrho_{vs})$ (*a*); relation (3.17) (*b*); $p_N(\varrho(0)) - p_N(\varrho_{vs})$ (*c*); $p(\varrho(0)) - p(\varrho_{vs})$ (*d*).

is non-uniform up to the centre of the drop, $p_N(0)$, $p_T(0)$ and $p(0)$ depart from p_l (see figure 2).

We multiply (2.6) by $\mu_h'(u)$ and integrate from a point deep inside the drop to one in the bulk vapour phase, thus obtaining

$$[\mu_h'^2(\varrho) - (\mu_h(\varrho) - \mu)^2 + 2\alpha p_h(\varrho)]_{\text{outside}} - [\mu_h^2(\varrho) - (\mu_h(\varrho) - \mu)^2 + 2\alpha p_h(\varrho)]_{\text{inside}}$$
$$= -\int_{\text{inside}}^{\text{outside}} \frac{4}{u}\mu_h'^2(u)\,\mathrm{d}u. \tag{3.16}$$

The quantity inside the brackets is equal to $(2\alpha p(\varrho))$ since $\mu_h'(u)$ vanishes at both limits; thus (3.16) may be written as

$$p_{\text{inside}} - p_{\text{outside}} = \int_{\text{inside}}^{\text{outside}} \frac{2}{\alpha u}\mu_h'^2(u)\,\mathrm{d}u. \tag{3.17}$$

This is a generalization of the Young–Laplace equation for a spherical dividing surface; the left-hand side is also considered as another possible definition of the pressure difference Δp.

Another important physical quantity is the surface tension $\gamma(R_\gamma; \Delta p)$ defined as the grand potential per unit surface area and depending on the dividing surface. Starting from its definition the surface tension $\gamma(R_\gamma; \Delta p)$, in reduced units, associated with a dividing surface with radius R_γ, is [8]

$$\gamma(R_\gamma; \Delta p) = -\frac{1}{R_\gamma^2}\int_0^\infty [p_h(u) - p_v - \tfrac{1}{2}\rho(u)(\mu - \mu_h(u))]u^2\,\mathrm{d}u + \tfrac{1}{3}R_\gamma \Delta p \tag{3.18a}$$
$$= -\frac{1}{2\alpha R_\gamma^2}\int_0^\infty \left[\int_u^\infty \frac{4}{t}\mu_h'^2(t)\,\mathrm{d}t - \mu_h'^2(u) - \left(\mu_h''(u) + \frac{2}{u}\mu_h'(u)\right)(\mu - \mu_h(u))\right]u^2\,\mathrm{d}u + \frac{1}{3}R_\gamma \Delta p \tag{3.18b}$$

on recalling (2.6). Integrating by parts the first and the third terms in the integrand in (3.18*b*), we find

$$\gamma(R_\gamma; \Delta p) = \frac{1}{3\alpha R_\gamma^2} \int_0^\infty (u\mu_h'(u))^2 \, du + \frac{1}{3} R_\gamma \Delta p. \tag{3.18c}$$

As radii R_γ we have chosen R_s, R_e and R_{max}.

The radius R_s can be found either by invoking its defining property (3.10*a*) or by combining the relations (3.10*b*) and (3.18*c*), thus finding

$$R_s^3 = \frac{2}{\alpha \Delta p} \int_0^\infty (u\mu_h'(u))^2 \, du. \tag{3.19}$$

In addition to R_s, another dividing surface is introduced through the requirement $\Gamma(R) = 0$, called the equimolar dividing surface [1, 6]; its radius, R_e, can be found from (3.9) by setting $\Gamma(R) = 0$,

$$R_e^3 = \frac{1}{\rho_{vs} - \rho_{ls}} \int_0^\infty r^3 \frac{d\rho(r)}{dr} \, dr. \tag{3.20}$$

Although the last two dividing surfaces, with radii R_s and R_e, are the ones mainly used, another dividing surface (with radius R_{max}) is also used, which relies only on the density profile itself.

The so-called mechanical route to the surface tension is defined through the relations (3.10*b*) and (3.19), while the thermodynamic route is defined through (3.10*b*), (3.20) and

$$R_s = \{3\gamma_\infty - [9\gamma_\infty^2 - 4\gamma_\infty R_e \Delta p]^{1/2}\}/\Delta p \tag{3.21}$$

which can be obtained from (3.10*b*) and (1.6) [1, 6, 11].

The curvature coefficient $C(R)$ (3.8*b*), on account of (3.17) and (3.18*c*), can be written as

$$C(R) = \frac{8\pi}{3\alpha R} \int_0^\infty u^2 \mu_h'^2(u) \left(\frac{R^3}{u^3} - 1 \right) du. \tag{3.22}$$

4. Results

4.1. Density profiles

The differential equation (2.11, 2.16) with the boundary conditions (2.13) was solved for various values of the bulk vapour density ϱ_{vs} (used to label the individual density profiles) at a fixed temperature for the calculation of the density profile. This equation was solved numerically for the reduced temperature $T^* = 0.8$ and various bulk vapour densities η_{vs} lying in the interval (η_{vc}, η_{vsp}), where η_{vc} is the coexisting vapour density and η_{vsp} is the corresponding spinodal density. All the relevant η_{vs}, together with the corresponding liquid densities η_{ls} and the densities $\eta(0)$ at the centre of the drop, are presented in table 1. The density profiles resulting as solutions to (2.11) are presented in figure 3; those of the larger drops represent a stable liquid in equilibrium with a metastable vapour and are similar to those of a planar interface at the same temperature; from these profiles one can ensure

the existence of a homogeneous phase inside the drop, in agreement with [6], [11], [14] and [15]. For each profile one can calculate the radius R_{hom} of a sphere, with the same centre as that of the drop under consideration, enclosing that part of the interior phase of the drop characterized by the constancy of its density, that is, it contains the homogeneous 'liquid' phase (figure 4); as long as R_{hom} is non-vanishing the interfacial zone separates two homogeneous regions, while for $R_{hom} \cong 0$ the spherical droplet contains an inhomogeneous fluid phase up to its centre, where, now, the local density is an unstable fluid, and the density profile fails to attain bulk values at the centre (see table 1); however, the symmetry condition, $\mu_h'(0) = 0$, still holds.

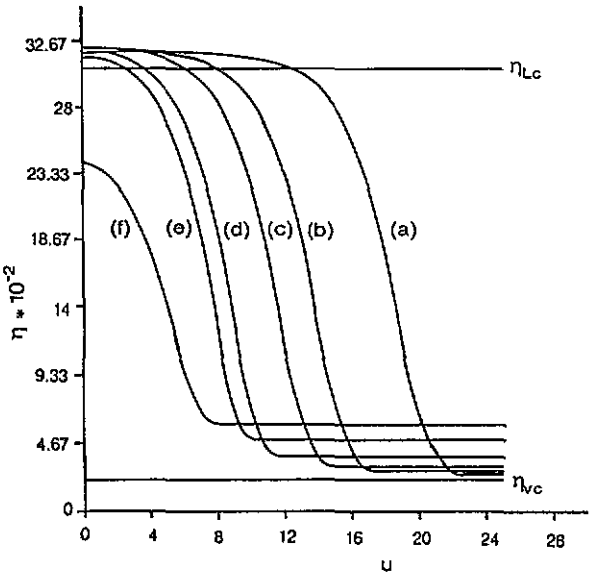

Figure 3. Density profiles for various drops labelled by the bulk vapour density ϱ_{vs} at $T^* = 0.8$ for $\varrho_{vs} = 0.5$ (*a*); 0.055 (*b*); 0.06 (*c*); 0.075 (*d*); 0;095 (*e*); 0.1166 (*f*). The upper and lower horizontal lines correspond to the planar interface liquid and vapour reduced coexistence densities, respectively.

As the density η_{vs} of the bulk vapour phase increases (or, equivalently, as the drop size decreases, see figure 5), the density $\eta(0)$ at the centre of the drop initially increases well above the liquid planar surface value $\eta_{lc} = 0.307\,211\,87$, as predicted by the Laplace equation, reaching a maximum value at about $\varrho_{vs} = 0.059\,489\,431$ (or, $\eta_{vs} = 0.031\,148\,593$ at $R_e = 9.101\,089$, $R_{max} = 12.001\,171$), then $\eta(0)$ starts decreasing as η_{vs} approaches η_{vsp} in agreement with [6], [11] and [14]. This behaviour of $\eta(0)$ is brought out in figure 6; a similar behaviour is also displayed by the pressure $p(0)$ at the drop centre, and by $p_N(0)$, as was seen earlier in figure 2, whre the different nature of these quantities for small drops can also be seen. For the larger drops the density $\eta(0)$ at the centre is nearly equal to the liquid density η_{ls} implied by bulk thermodynamics, while for the smaller droplets $\eta(0)$ departs considerably from η_{ls} (this is brought out by figure 7; see also table 1).

The average drop size can also be expressed by the number of particles N_{drop} contained in the drop,

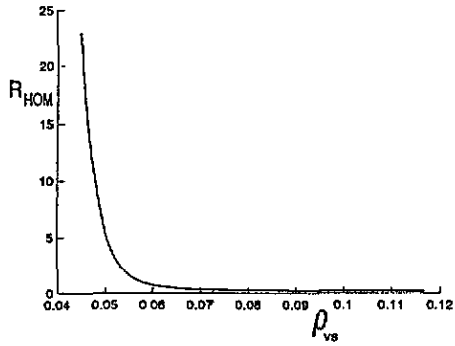

Figure 4. The radius R_{hom} of the sphere containing a uniform fluid for the density profiles in figure 3 against bulk vapour density ϱ_{vs}.

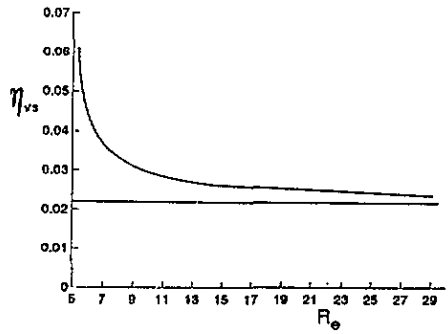

Figure 5. The bulk vapour density η_{vs} against equimolar radius R_{e}. The horizontal line corresponds to the vapour density for the planar interface at the same temperature, $T^* = 0.8$.

$$N_{\text{drop}} = 4\pi \int_0^{R_{10}} \varrho(r) r^2 \, \mathrm{d}r \tag{4.1}$$

where R_{10} is the distance (radius) from the centre of the drop such that

$$\varrho(R_{10}) = \varrho_{\text{vs}} + 0.1(\varrho_{\text{ls}} - \varrho_{\text{vs}}). \tag{4.2}$$

4.2. Pressure tensors

Once the density profiles have been calculated, the pressure tensor components $p_{\text{N}}(u)$ and $p_{\text{T}}(u)$ can be evaluated from the expressions (3.7) and (3.13), respectively, and their profiles are displayed in figure 8 for a sequence of increasing supersaturation.

For the larger drops (small supersaturations) both components $p_{\text{N}}(u)$ and $p_{\text{T}}(u)$ cioncide over a distance inside the drop reflecting the existence of a bulk-like liquid phase inside the drop. However, within the transition region the two components are separated from each other; the transverse component $p_{\text{T}}(u)$ becomes smaller than the normal $p_{\text{N}}(u)(p_{\text{T}}(u) < p_{\text{N}}(u))$, so that the interface is under tension and $p_{\text{T}}(u)$ displays a deep lobe, which for the smaller supersaturations acquires a negative part. Another characteristic of their profiles (more pronounced in small supersaturations) is the existence of a small part of the interface under compression $(p_{\text{T}}(u) > p_{\text{N}}(u))$ that disappears in larger supersaturations. In the outer region of the interface, inside the bulk vapour phase, both tensors join smoothly together to their common value, which coincides with the bulk vapour pressure p_{v}, i.e., $p_{\text{T}}(\infty) = p_{\text{N}}(\infty) = p_{\text{v}}$. This overall behaviour of $p_{\text{N}}(u)$ and $p_{\text{T}}(u)$, for the larger drops, is in accordance with the MD simulations of Thompson *et al* [6], Nijmeijer *et al* [15] and the numerical calculations of Falls *et al* [14]. As the supersaturation is increased further towards the spinodal density, there is no portion of the interior of these small droplets where the two components $p_{\text{T}}(u)$ and $p_{\text{N}}(u)$ coincide, except at the centre of the droplet (where they coincide by symmetry), because inside these small droplets there is no region that can be considered as bulk like (a similar behaviour was found earlier in the density profiles). As the supersaturation is decreased towards the planar interface limit, the drops become larger and larger; the pressure difference Δp is reduced so that in the limit of a planar interface $p_{\text{N}}(x)$ attains a constant value equal to the bulk pressure, $p_{\text{N}}(x) = p(\varrho_{\text{vc}}) = p_{\text{flat}}$,

Table 1. ρ_{vs}^*, bulk vapour density; R_s^*, mechanical radius of the surface of tension with γ_s^* the associated surface tension; R_{max}^*, radius of the sphere where $|dq(u)/du|$ is maximum with γ_{max}^* the associated surface tension; R_e^*, equimolar radius with γ_e^* the associated surface tension; η_{vs}^*, η_{ls}^*, bulk vapour and corresponding liquid packing fraction, respectively; $\eta^*(0)$, packing fraction at the centre of the drop; N_{drop}, number of particles in the drop; R_{hom}^*, radius of sphere containing the homogeneous phase inside the drop.

ρ_{vs}^*	γ_s^*	R_s^*	γ_{max}^*	R_{max}^*	γ_e^*	R_e^*	η_{vs}^*	$\eta^*(0)$	η_{ls}^*	N_{drop}	R_{hom}^*
0.044	0.450 75	48.730 710	0.450 77	49.134 447	0.474 36	39.121 639	0.023 04	0.312 000	0.312 00	286 475	34.434 944
0.045	0.456 04	36.390 532	0.456 11	36.846 480	0.480 07	29.197 645	0.023 56	0.312 473	0.312 47	119 920	23.008 210
0.050	0.482 12	18.055 185	0.482 41	18.505 050	0.507 51	14.486 850	0.026 18	0.318 055	0.318 25	15 130	5.484 630
0.055	0.503 32	13.213 179	0.504 08	13.740 349	0.529 27	10.625 573	0.028 80	0.321 003	0.322 67	6 138	1.628 486
0.060	0.518 12	10.946 735	0.519 43	11.515 125	0.544 23	8.823 8394	0.031 42	0.321 718	0.326 13	3 601	0.748 480
0.065	0.527 04	9.629 458	0.528 97	10.236 864	0.553 19	7.774 3257	0.034 03	0.321 182	0.328 90	2 516	0.462 974
0.075	0.532 33	8.182 411	0.535 66	8.865 174	0.558 59	6.609 849	0.039 27	0.318 812	0.332 90	1 604	0.288 840
0.085	0.528 28	7.441 089	0.532 95	8.186 171	0.554 74	6.001 928	0.044 51	0.316 482	0.335 47	1 238	0.243 757
0.095	0.520 13	7.029 229	0.525 90	7.823 899	0.546 735	5.657 308	0.049 74	0.314 859	0.337 07	1 062	0.210 938
0.100	0.515 29	6.897 915	0.521 34	7.702 426	0.541 926	5.545 445	0.052 36	0.314 333	0.337 58	1 011	0.206 650
0.105	0.510 11	6.802 240	0.516 65	7.633 659	0.536 754	5.462 709	0.054 98	0.313 977	0.337 93	976	0.203 318

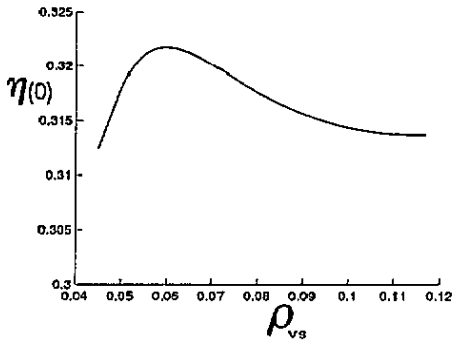

Figure 6. The variation of the density at the origin of the drop, $\eta(0)$, with the bulk vapour density ϱ_{vs}.

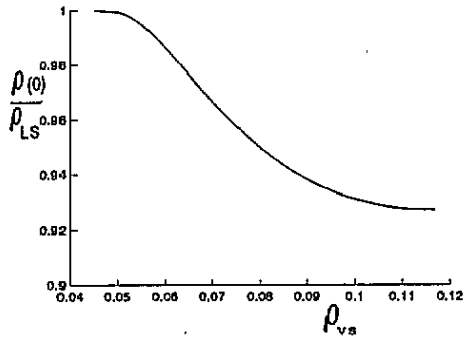

Figure 7. The ratio of the actual density at the drop centre ($\varrho(0)$) to that predicted by bulk thermodynamics (ϱ_{ls}) against bulk vapour density (ϱ_{vs}).

while $p_T(x)$ varies with distance according to (3.11, 13) and displays a large negative part in the interfacial region, which is mainly smaller than $p_N(x)$ (interface under tension) but ultimately it joins smoothly with $p_N(x)$, although on the vapour side of the profile there exists a small region where $p_T(x) > p_N(x)$ (interface under compression), (see figure 9); this behaviour was also found in [14] and [16]–[19] for the Irving–Kirkwood (IK) version of the pressure tensor but not for the Harasima (H) version.

The surface tension (3.18*c*) and the two radii (3.19, 21) of the surface of tension depend explicitly on the pressure difference Δp (R_e and R_{max} do not depend on Δp), which in non-planar geometries is an ill defined quantity but connected with the chemical potential through the Gibbs–Duhem relation $\delta p = \varrho \delta \mu$ (at constant temperature; in planar geometries Δp is identically zero). In general, Δp can be defined in various ways [6, 14, 15, 21]: by the expression (3.17), by subtracting the bulk pressure p_v from that at the origin of the drop $p(0)$, or subtracting $p_N(\varrho_{vs}) = p_v$ from $p_N(0)$, or $p(\varrho_{vs}) = p_v$ from $p(\varrho_{ls}) = p_l$ (figure 2). However, for large drops, the pressures $p(\varrho_{ls})$, $p(0)$, and $p_N(0)$ are equal; as a consequence, the corresponding Δp-curves coincide for these drops and do not deviate considerably when the supersaturation is still small; however the deviation is significant for the smaller drops (high supersaturation). The pressure $p(r)$ (2.18*b*) is a monotonic function of density and the pressure p_v of the bulk phase does not vary significantly, so the corresponding Δp-curves exhibit the same behaviour as those of $p(0)$, $p_N(0)$, and $p(\varrho_{ls}) = p_l$, respectively.

The density ϱ_{vs} increases from ϱ_{vc} to ϱ_{vsp}; so does ϱ_{ls} (both are solutions of the equation $\mu(\varrho) - \mu = 0$), and p_l is an increasing function of ϱ_{ls}; the other two quantities $p_N(0)$ and $p(0)$ attain a maximum value, which reflects the non-monotonic behaviour of $\varrho(0)$ (see figure 6). For large drops (when ϱ_{vs} is close to ϱ_{vc}) p_l, $p_N(0)$, and $p(0)$ are equal or nearly equal, while for smaller drops they depart and $p_N(0) > p(0)$ because $p_T(0) = p_N(0) = p(0) + \frac{1}{2}(\mu - \mu(0))$ and $\mu > \mu(\varrho(0))$ for real densities.

In the integral expression (3.17) for Δp, the integrand vanishes inside the bulk vapour (exterior) phase, since, in this region, $\mu_h'(u)$ is zero identically, thus the contribution to the integral in (3.17) originates solely from the interior and interfacial regions and this causes Δp to increase (the integrand is positive and the density profile is steeper for the smaller drops).

The four definitions for Δp are independent from each other in the sense that the integral definition monitors the behaviour of the derivative of the hard-sphere chemical potential inside the drop and in the interface, while the other three extract Δp either from

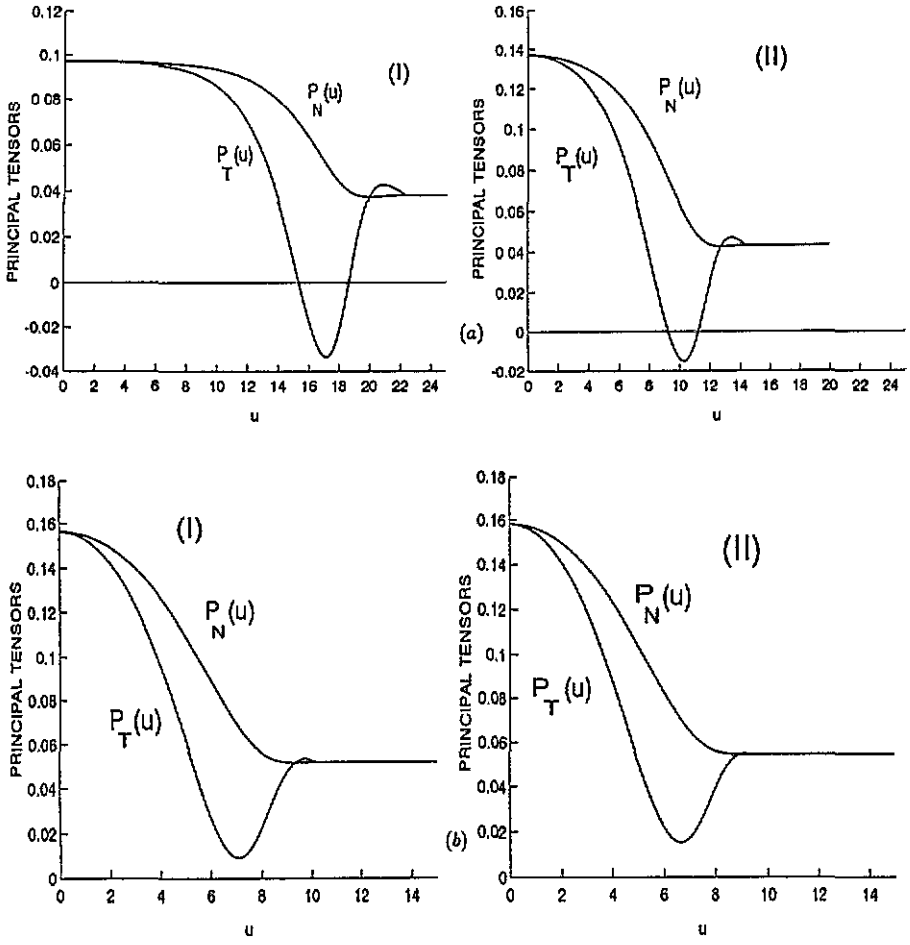

Figure 8. (*a*) (I) Pressure tensor components $p_N(u)$ and $p_T(u)$ against reduced distance from the centre of the drop for reduced density $\varrho_{vs} = 0.05(\eta_{vs} = 0.02618)$. (II) Pressure tensor components for $\varrho_{vs} = 0.06(\eta_{vs} = 0.031416)$. (*b*) (I) Pressure tensor components for $\varrho_{vs} = 0.085(\eta_{vs} = 0.0445)$. (II) Pressure tensor components for $\varrho_{vs} = 0.1(\eta_{vs} = 0.05236)$.

the pressure itself or the pressure tensor in the 'bulk' phases.

For the calculation of $\gamma(R_\gamma; \Delta p)$ and R_s, Δp is chosen to be given by (3.17), because this expression depends on the global behaviour of the system and not on specific points; this is also valid for small drops, where the interior phase is no longer bulk like and does not possess a plateau and the density $\varrho(0)$ deviates significantly from the ϱ_{ls} implied by bulk thermodynamics (which assumes a bulk-like interior phase). As the supersaturation is increased from the planar vapour value (i.e., starting from very large drops) the tension increases slowly from its planar value up to a maximum value (see table 1 and figure 10), which occurs around $R_\gamma \cong 8$ when R_γ is taken to be R_s or R_{max}, and $R_\gamma \cong 6$ when R_γ is taken to be R_e; later it decreases rapidly as the size of the drop decreases, in agreement with simulation [6] and other numerical calculations [11, 14, 20]; this non-monotonic behaviour in $\gamma(R_\gamma; \Delta p)$ was observed earlier only in [10]. The initial increasing tendency of $\gamma(R_\gamma; \Delta p)$ is similar to that of the density at the centre of the drop, $\varrho(0)$, which also attains a maximum value (in this range of densities, the drop formed is large); this increase in density implies

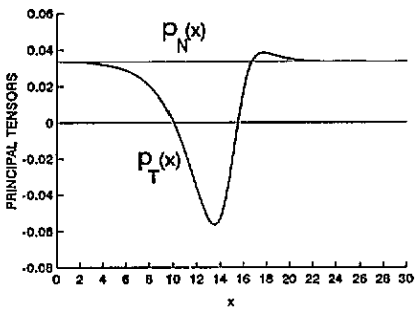

Figure 9. Flat interface pressure tensor components $p_N(x)$ and $p_T(x)$ against reduced distance.

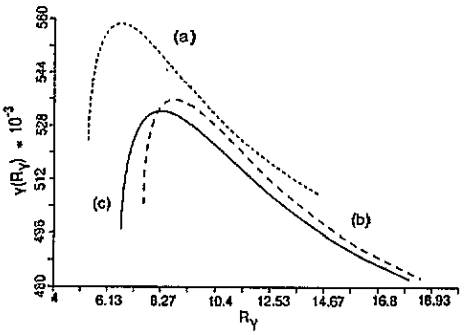

Figure 10. Surface tension $\gamma(R_\gamma)$ against drop radius R_γ: γ_e against R_e (*a*); γ_{max} against R_{max} (*b*); γ_s against R_s (*c*) (calculated via the mechanical route). Δp was set to that of (3.17).

accumulation of particles in the neighbourhood of the centre of the drop, resulting in increasing surface tension. For the smaller drops, where the density is non-uniform up to the centre, the value of the surface tension does not deviate very much from that of γ_∞ and, as long as the overall behaviour of tensions is the same, γ_{max} can be used as a measure of the surface tension of drops of any size.

The asymptotic behaviour of Δp is described by the formula (see [6])

$$\lim_{R_e \to \infty} \Delta p = 2\gamma_\infty / R_e \tag{4.3}$$

and this appears in figure 11 together with the correct form of Laplace equation (1.2) calculated through the mechanical route. For small drops the asymptotic form (4.4) deviates from the correct Laplace equation, giving larger Δp, while for the larger drops both formulae give nearly the same results (see [6] and [14]).

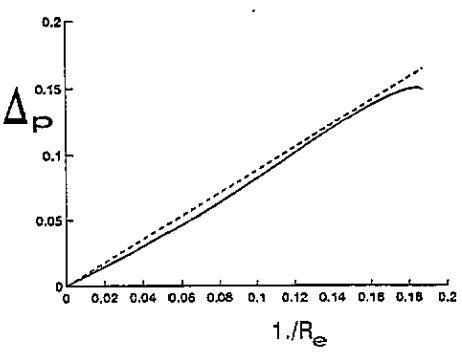

Figure 11. The pressure difference as a function of $(1/R_e)$ as deduced from the correct form of the Laplace equation (full line) and from the asymptotic form (dashed line).

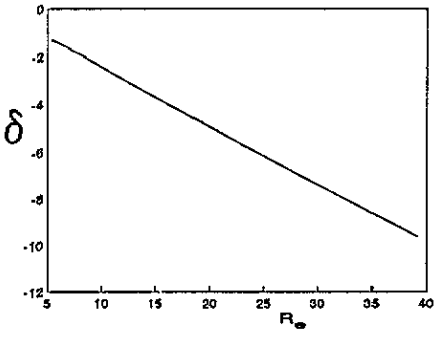

Figure 12. Tolman's length δ against equimolar radius R_e.

In figure 12 we plot Tolman's length $\delta = R_e - R_s$ (see table 1, calculated through the mechanical route (3.10*b*, 19)) as a function of the equimolar dividing radius R_e. Tolman's

length δ is negative (an expected result since the surface tension γ_s is greater than γ_∞) and strongly drop dependent, thus the surface of tension is on the gas side of the equimolar surface; a similar behaviour of δ was observed in [10] and [13], while in [6], [11] and [14] δ was found to be is positive and tend to zero as $R_e \to \infty$. Nijmeijer *et al* [15] have done MD simulations on a similar system at $T^* = k_B T/\epsilon = 0.9$, finding that the data for δ is scattered around zero, and concluded that $|\delta^*| < 0.7$; this result was also verified by Blokhuis and Bedeaux [21]. In the limit $R_e \to \infty$, for the transition from the spherical interface to the planar, one expects to find δ negative since the liquid–vapour interface (figure 1) is not symmetric (the vapour branch of the density profile is steeper than the liquid branch) thus $z_e \neq z_s$ ([31]; see (3.19) and (3.20); for planar interfaces see [17], [18] and [22]).

The distribution of matter in the interface can be better described by adsorption (3.9) as a function of the distance from the centre of the drop (figure 13) for various bulk vapour densities ϱ_{vs}. For small distances from the centre of the drop adsorption varies slowly, in the interfacial region it varies significantly, but for larger distances, within the bulk phase, it becomes negative and varies slowly. The respective adorption curves cut the radius axis at a point identical to R_e.

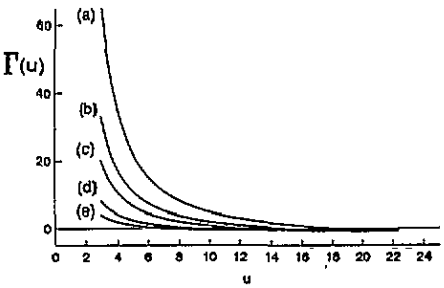

Figure 13. Adsorption $\Gamma(R)$ as a function of the distance from the origin of the drop for various bulk vapour densities ϱ_{vs}: 0.05 (*a*); 0.052 (*b*); 0.055 (*c*); 0.065 (*d*); 0.085 (*e*).

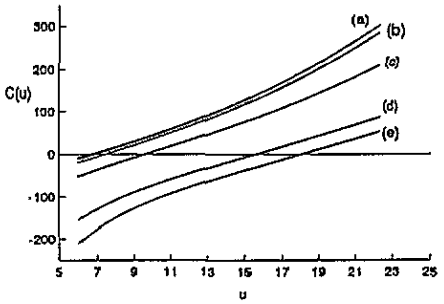

Figure 14. The curvature term $C(R)$ as a function of the distance from the origin of the drop for various bulk vapour densities ϱ_{vs}: 0.1 (*a*); 0.085 (*b*); 0.065 (*c*); 0.052 (*d*); 0.05 (*e*).

In figure 14 we present the plots of the curvature term $C(R)$ (see (3.8*b*)) for various bulk vapour densities; each curve cuts the radius axis at a point that coincides with R_s (the radius of the surface of tension (3.19)).

5. Conclusions

We have studied the interfacial properties and stresses of liquid drops of various radii embedded in a vapour background using Sullivan's model at reduced temperature $T^* = 0.8$. The advantage of this model over other models is that it can be described by a non-linear differential equation instead of an integral equation; this was solved numerically for various values of the bulk vapour density ϱ_{vs}. The numerical results of this mean field theory are compared with the numerical and MD simulations for other model fluids [6, 10, 11, 13–15, 21] expecting only qualitative agreement.

As ϱ_{vs} increases from ϱ_{vc} towards ϱ_{vsp}, the drop size decreases; initially, the distribution of particles around the centre of the drop is constant, implying the existence of a

homogeneous phase inside the drop (as required by bulk thermodynamics), but this disappears gradually as the drop size decreases further so that the interior phase becomes non-uniform up to the centre of the drop; however, parallel to this behaviour of the interior phase, the density at the drop centre initially increases, but later decreases, and departs increasingly from the density ϱ_{ls} predicted by bulk thermodynamics. These results are in qualitative agreement with the numerical and MD calculations referred to above.

A striking result of this mean field theory calculation is the non-monotonic behaviour of the surface tension as ϱ_{vs} increases, in contrast to the monotonic behaviour shown, in general, by $\gamma(R)$ (the only exception is in [10]). Another quantity related to the surface tension is Tolman's length δ, which has caused much debate. The δ obtained by mean field theory is negative and it seems to be such in the planar interface limit $R_e \to \infty$. In the two main routes to the surface tension, the pressure difference Δp is involved; this quantity, although is independent of the dividing surface, displays a significant drawback, it is not uniquely defined in the sense that it can be defined in various ways independently and their results are identical only for large drops.

In conclusion, some of our results agree, qualitatively as expected, with those of other models and approximations, but some others do not, e.g., the surface tension, Tolman's length, Δp, pressure tensor; more MD simulations and experiments on real systems could resolve some of the problems.

Acknowledgments

The author expresses his gratitude to Professor R Evans (University of Bristol) for his beneficial comments and to Professor G J Papadopoulos and Dr S Messoloras for useful discussions.

References

[1] Rowlinson J S and Widom B 1982 *Molecular Theory of Capillarity* (Oxford: Clarendon)
[2] Sullivan D E and Telo da Gama M M 1986 *Fluid Interfacial Phenomena* ed C A Croxton (New York: Wiley) ch 2
[3] Dietrich S 1988 *Phase Transitions and Critical Phenomena* vol 12, ed C Domb and J L Lebowitz (London: Academic) ch 1
[4] Tolman R C 1948 *J. Chem. Phys.* **16** 758; 1949 *J. Chem. Phys.* **17** 118, 333
[5] Rowlinson J S 1992 *Fundamentals of Inhomogeneous Fluids* ed D Henderson (New York: Dekker) ch 1
[6] Thompson S M, Gubbins K E, Walton J P R B, Chantry R A R and Rowlinson J S 1984 *J. Chem. Phys.* **81** 530
[7] Evans R 1990 *Liquids at Interfaces (Les Houches Session XLVIII)* ed J Charvolin, J F Joanny and J Zinn-Justin (Amsterdam: Elsevier) ch 1; 1992 *Fundamentals of Inhomogeneous Fluids* ed D Henderson (New York: Dekker) ch 3
[8] Sullivan D E 1979 *Phys. Rev.* B **20** 3991; 1981 *J. Chem. Phys.* **74** 2604
[9] Stoer J and Bulirsch R 1983 *Introduction to Numerical Analysis* (New York: Springer)
[10] Guermeur R, Biquard F and Jacolin C 1985 *J. Chem. Phys.* **82** 2040
[11] Lee D J, Telo da Gama M M and Gubbins K E 1986 *J. Chem. Phys.* **85** 490
[12] Schofield P and Henderson J R 1982 *Proc. R. Soc.* A **379** 231
[13] Hemingway S J, Henderson J R and Rowlinson R S 1981 *Faraday Symp. Chem. Soc.* **16** 33
[14] Falls A H, Scriven L E and Davis H T 1981 *J. Chem. Phys.* **75** 3986
[15] Nijmeijer M P J, Bruin C, van Woerkom A B, Bakker A F and van Leeuwen J M J 1992 *J. Chem. Phys.* **96** 565
[16] Rowlinson J S 1983 *Chem. Soc. Rev.* **12** 251
[17] Lee D J, Telo da Gama M M and Gubbins K E 1984 *Mol. Phys.* **53** 1113

[18] Walton J P R B, Tildesley D J and Rowlinson J S 1983 *Mol. Phys.* **48** 1357
[19] Davis H T and Scriven L E 1982 *Adv. Chem. Phys.* **49** 357
[20] Hooper M A and Nordholm S 1984 *J. Chem. Phys.* **81** 2432
[21] Blokhuis E M and Bedeaux D 1992 *J. Chem. Phys.* **97** 3576
[22] Rao M and Berne B J 1979 *Mol. Phys.* **37** 455
[23] Baus M and Lovett R 1990 *Phys. Rev. Lett.* **65** 1781; 1991 *Phys. Rev.* A **44** 1211
[24] Rowlinson J S 1991 *Phys. Rev. Lett.* **67** 406
[25] Baus M and Lovett R 1991 *Phys. Rev. Lett.* **67** 407
[26] Lovett R and Baus M 1993 *Physica* A **194** 93
[27] Henderson J R 1986 *Fluid Interfacial Phenomena* ed C A Croxton (New York: Wiley) ch 12
[28] Sullivan D E 1982 *J. Chem. Phys.* **77** 2632
[29] Telo da Gama M M and Evans R 1983 *Mol. Phys.* **48** 687
[30] Hadjiagapiou I and Evans R 1985 *Mol. Phys.* **54** 383
[31] Fisher M P A and Wortis M 1984 *Phys. Rev.* B **29** 6252